American Mineralogist, Volume 72, pages 566–579, 1987

Experimental study of hydrogen-isotope exchange between aluminous chlorite and water and of hydrogen diffusion in chlorite

COLIN M. GRAHAM
Department of Geology, Edinburgh University, Edinburgh, EH9 3JW, Scotland
JANET A. VIGLINO, RUSSELL S. HARMON
Department of Geological Sciences, Southern Methodist University, Dallas, Texas 75275, U.S.A.

ABSTRACT

Hydrogen-isotope exchange between Mg-Al chlorite of sheridanite composition and water has been studied experimentally over the temperature range 300–700°C. Problems were encountered with changes in the bulk D/H ratios of capsule contents during high *P-T* experiments. Below 500°C, exchange was so slow that equilibrium fractionation factors could not be determined. Over the temperature range 500–700°C, no temperature dependence is observed, with 1000 ln $\alpha^{e}_{\text{chl-H}_2\text{O}}$ around −28. Chlorite-water fractionations are not simply related to octahedral cation composition; preferential fractionation of the light isotope into chlorite reflects the presence of hydrogen bonding in the chlorite structure.

A compilation of experimentally and empirically determined chlorite-water hydrogen-isotope fractionation factors over a wide range of temperatures indicates that these are not measurably dependent on Fe/Mg in chlorite.

Hydrogen-isotope exchange reactions proceeded by volume diffusion of hydrogen in chlorite, for which activation energies in the range 166–172 kJ/mol H are much higher than in any other hydrous mineral yet studied. Hydrogen-isotope exchange between chlorite and water in slowly cooling metamorphic rocks may nonetheless proceed to subgreenschist facies temperatures.

Hydrogen-isotope exchange during hydrous metamorphism of the oceanic crust in the temperature range 200–500°C may be dominated by fractionation factors in the range 1000 ln $\alpha^{\text{D-H}}_{\text{chl-water}} = -30$ to −40.

INTRODUCTION

Studies of hydrogen- and oxygen-isotope variations in rocks and minerals provide a powerful method of documenting fluid-rock interactions in the Earth's crust (Taylor, 1974; Sheppard, 1977). The hydrogen-isotope compositions of hydrous minerals are particularly sensitive indicators of the isotope composition of the last fluid with which they have equilibrated, because (1) most hydrous minerals contain relatively small amounts of hydrogen relative to infiltrating hydrous fluids unless fluid/rock ratios were very small, (2) waters of different origins in the Earth's crust and hydrosphere have distinctive hydrogen-isotope composition, and (3) hydrogen-isotope exchange between hydrous minerals and water should be relatively fast during mineral-water interactions and crystallization of hydrous minerals. In order to calculate the isotope composition of a fluid phase that has subsequently been removed from a water-rock system, it is necessary to know the isotope fractionation factors between hydrous minerals and water as a function of temperature and mineral composition.

In this paper, we report the results and applications of an experimental study of hydrogen-isotope fractionation between aluminous chlorite and water and of rates for hydrogen diffusion in chlorite, at high pressures (2–5 kbar) and over a range of temperatures (300–700°C) representative of a spectrum of metamorphic conditions and some hydrothermal environments. Aluminous chlorites are common and abundant constituents of a wide range of crustal rock types crystallizing in these hydrous environments. Chlorites, with about 12 wt% water, contain the majority of structural water present in many low-grade metamorphic and hydrothermal rocks, most importantly in hydrated mafic oceanic crust. Therefore the results of the study should provide new data applicable to the determination of the stable isotope compositions and origins of hydrous fluids in a variety of crustal geologic environments.

Preliminary results of this experimental study have been reported in abstract form by Viglino et al. (1984) and Graham et al. (1984b). No other experimental data are available on hydrogen-isotope exchange between chlorite

0003–004X/87/0506–0566$02.00

TABLE 1. Chemical analyses of chlorite 94515

	1	2
SiO_2	29.79	28.81
Al_2O_3	25.54	26.43
TiO_2	0.06	—
Fe_2O_3	—	0.24
FeO	0.34	0.40
MgO	32.29	31.21
MnO	0.01	—
K_2O	—	0.35
Na_2O	—	0.14
H_2O*	12.40	13.89
Total	100.43	101.47
Si	5.51	5.23
Al	5.57	5.66
Ti	0.01	—
Fe^{3+}	—	0.03
Fe^{2+}	0.05	0.06
Mg	8.90	8.45
Mn	—	—
K	—	0.08
Na	—	0.05
OH	15.31	16.84

Note: Columns are (1) Jones (1981). X-ray fluorescence and colorimetry analysis. Water content determined by weight loss to 1000°C during DTA experiments. (2) Shannon and Wherry (1922). Wet-chemical analysis.

* H_2O content of starting material, determined by induction heating in this study, is 12.95%.

TABLE 2. Isotope compositions of starting materials

	δD^i (‰)	$10^3(\alpha_i - 1)$
Chlorite 94515	−33.5	—
Water 1	6.4	−39.6
Water 2	3.4	−36.8
Water 3	−26.5	−7.2
Water 4	−50.8	18.2

Note: α_i is the initial (uncorrected) chlorite-water fractionation factor.

and water, although data on hydrogen-isotope exchange between serpentine and water (Suzuoki and Epstein, 1976; Sakai and Tsutsumi, 1978) and brucite and water (Satake and Matsuo, 1984) have been reported. The serpentine and brucite data are relevant to this study because both serpentine and chlorite are sheet silicates, with brucite layers incorporated in the sheet structure, and serpentine is chemically similar to Al-free chlorite.

Empirical estimates of hydrogen-isotope fractionation factors for the chlorite-water system as a function of temperature and Fe/Mg ratio in chlorite have been made using isotope data for chlorites from pelitic schists (Taylor, 1974; Kuroda et al., 1976), hydrothermal ore deposits (Kuroda et al., 1976) and drill-core samples from a recent geothermal field (Marumo et al., 1980). These empirical calibrations are usually based on assumptions regarding the hydrogen-isotope composition of the water with which the minerals have equilibrated, the temperature of crystallization of the chlorites, and the absence of retrograde re-equilibration of the chlorite with hydrous fluid. These assumptions may be poorly founded, especially because many hydrous minerals will readily exchange hydrogen with water to temperatures well below those of primary crystallization during slow cooling (Graham, 1981). Therefore, empirical calibrations of hydrogen-isotope fractionation factors not derived from direct experimental calibration must be treated with caution.

Experimental measurement of rates of hydrogen-isotope exchange between chlorite and water in this study permits calculation of rates of hydrogen diffusion in chlorite. These diffusion rates may be compared with rates of hydrogen diffusion in other hydrous minerals (Graham, 1981; Graham et al., 1984a) and may be used to calculate closure temperatures for cessation of hydrogen-isotope exchange between chlorite and water in slow-cooling geologic environments.

STARTING MATERIALS

The chlorite used in this study is a sheridanite (specimen number 94515, Smithsonian Institution Museum of Natural History, Washington, D.C.) whose composition is shown in Table 1. This chlorite is comparably aluminous to typical chlorites in low-grade aluminous metamorphic and hydrothermal rocks (Velde and Rumble, 1977). Optical, XRD, and SEM examination showed the sample to be free of contamination.

The specimen was prepared by grinding and sieving to obtain sized starting materials with nominal grain-size fractions of <44 μm (fine), 44–63 μm (medium), and 63–105 μm (coarse). The finest material was removed from the fine grain-size fraction by elutriation.

The isotope compositions of the chlorite and the waters used as starting materials in this study are given in Table 2. The isotope compositions of the waters were chosen so that hydrogen-isotope equilibrium between chlorite and water would be approached by exchange from two directions during experiments (cf. Suzuoki and Epstein, 1976; Graham et al., 1980). All mineral-water charges were sealed into separate capsules as part of the same batch, in order to circumvent problems arising from variation of starting water composition with time and to ensure internal consistency of data (cf. Graham et al., 1980).

EXPERIMENTAL AND ANALYTICAL METHODS

Experimental and analytical methods are comparable to those described by Graham et al. (1980, 1984a). Exchange runs were made in Au capsules of 5 mm O.D. × 0.5 mm wall × 20 mm (approx.) length. Each run typically contained 125-mg chlorite and 16-mg water, capsules and mineral powders having been stored and dried at 110°C prior to loading in order to minimize adsorption of atmospheric moisture. Runs were made in Nimonic-105 cold-seal pressure vessels (2-kbar runs) and internally heated gas-pressure vessels (5-kbar runs) using an Ar pressure medium. After quenching, capsules were weighed to check for leakage, heated at 120°C overnight under vacuum to remove adsorbed moisture, and then pierced under vacuum to release free water that was collected by freezing into a liquid-N_2 cold trap while heating capsules at 120°C for up to 4 h to ensure removal of all free water. Hydrogen gas formed by passage of this water over hot U was measured manometrically to further ensure complete removal and collection of free water.

TABLE 3. Results of hydrogen-isotope exchange experiments for the system chlorite-H_2O

Run	Grain size*	T (°C)	P (kbar)	Time (s × 10^5)	Δ	$10^3 \times (\alpha_i' - 1)$**	δD^f_{chl}	$\delta D^f_{H_2O}$	$10^3 \times (\alpha_f - \alpha_i)$	$10^3 \ln \alpha_f$	$10^3 \ln \alpha^e$	f	log K_2	log D_{cyl}	log $D^{(1)}_{plate}$	log $D^{(2)}_{plate}$
23	M	700	5	0.96	+2.6	−37.16(1)*	−27.4	3.0	6.89	−30.78	−28.96 ± 1.7	0.793	−4.400	−14.54	−15.70	−16.30
22	M	700	5	0.96	+0.5	18.76(4)	−50.9	−32.5	−37.82	−19.20		0.799	−4.385	−14.53	−15.70	−16.30
31	C	700	5	1.21	+1.5	−38.12(1)	−27.9	2.2	8.07	−30.49	−27.20 ± 2.0	0.717	−4.678	−14.43	−15.75	−16.36
35	C	700	5	1.21	+2.6	−4.74(3)	−38.9	−18.8	−15.79	−20.70		0.715	−4.682	−14.42	−15.74	−16.35
3	F	600	2	40.18	+3.2	0.0(2)	−28.4	1.5	—	−30.31	−29.80 ± 1.4	1.0	—	—	—	—
2	F	600	2	40.18	+49.6	0.0(3)	−19.7	9.5	—	−29.35		1.0	—	—	—	—
17	M	600	2	2.55	−6.1	−42.59(2)	−35.0	−1.2	8.76	−34.43	−26.09 ± 2.4	0.524	−5.365	−15.52	−16.63	−17.23
16	M	600	2	2.55	−5.0	12.89(4)	−48.6	−41.7	−20.10	−7.23		0.519	−5.373	−15.51	−16.62	−17.22
24	C	600	2	2.55	+6.7	25.50(4)	−41.2	−36.8	−30.07	−4.58		0.566	−5.291	−15.04	−16.34	−17.94
6	F	500	2	5.267	−10.7	−46.94(2)	−39.4	−1.3	8.8	−38.84	−28.58 ± 3.1	0.471	−5.777	−16.96	−18.10	−18.70
5	F	500	2	5.267	−2.4	−9.63(3)	−40.2	−22.3	−8.7	−18.47		0.468	−5.772	−16.97	−18.10	−18.70
11	F	500	2	37.05	+3.5	−3.61(3)	−39.5	−17.0	−19.30	−23.17		0.798	−5.972	−17.12	−18.33	−18.93
19	M	500	2	22.52	−2.7	−36.36(2)	−33.6	0.8	5.02	−34.98	−27.78 ± 3.3	0.417	−6.498	−16.74	−17.82	−18.42
18	M	500	2	22.52	−5.3	12.57(4)	−46.8	−42.8	−16.78	−4.19		0.420	−6.493	−16.72	−17.81	−18.41
27	C	500	2	37.19	−5.1	−41.65(2)	−34.4	−0.8	7.97	−34.21	−20.87 ± 3.7	0.383	−6.777	−16.67	−17.94	−18.54
26	C	500	2	37.19	−1.4	16.73(4)	−41.8	−44.2	−14.19	2.51		0.380	−6.784	−16.68	−18.33	−18.54
9	F	400	2	135.65	+1.9	−34.95(2)	−34.8	6.6	−6.23	−42.00		—	—	—	—	—
28	C	400	2	90.72	−4.1	13.86(4)	−36.8	−51.7	1.81	15.59		0.04	—	—	—	—
15	F	300	2	135.65	−0.8	−40.39(1)	−35.8	8.0	−3.05	−44.42	—	—	—	—	—	—
32	F	300	2	135.65	−5.7	−12.96(3)	−35.7	−30.0	7.13	−5.89		—	—	—	—	—
13	F	300	2	135.65	−4.4	13.42(4)	−34.9	−53.9	6.68	19.88		—	—	—	—	—

Note: Δ = mass-balance value (calculated using Eq. 5; see text for discussion); α_i' = initial fractionation factor, after correction for exchange of hydrogen between water in capsule and pressure medium, using mass-balance values (Δ) calculated using Eq. 5 (see text for discussion); α_f = final fractionation factor; α^e = equilibrium fractionation factor; δD^f = hydrogen-isotope compositon after exchange; values of α^e interpolated from partial-exchange experiments (see text); f = fractional approach to equilibrium = $(\alpha_f - \alpha_i)/(\alpha^e - \alpha_i)$; K_2 = rate constant for second-order exchange reaction; D_{cyl} = diffusion coefficient ($m^2 \cdot s^{-1}$) from cylinder model; D_{plate} = diffusion coefficient ($m^2 \cdot s^{-1}$) from plate model using measured grain thickness (1) or adjusted grain thickness (2) (see Table 6). 5-kbar experiments conducted in internally heated gas vessels; 2-kbar experiments conducted in cold-seal pressure vessels.

* F = fine-grained chlorite; M = medium-grained chlorite; C = coarse-grained chlorite (see Table 6).

** Value in parentheses indicates starting water used (see Table 2).

Chlorite run products were washed with distilled water and examined optically and by XRD and SEM to check for absence of mineral alteration and thermal decomposition. For isotope analysis, 20–30 mg of chlorite were loaded into previously outgassed Mo (at Southern Methodist University) or Pt (at Scottish Universities Research and Reactor Centre) crucibles heated under vacuum at 120°C overnight to remove adsorbed moisture. Structural water was released by induction heating for about 1 h, and hydrogen yields after conversion by passage over hot U were measured manometrically to check water contents of chlorite for consistency with initial values and to ensure complete removal of structural water.

D/H ratios in waters and chlorites were measured on a Finnegan MAT 251 mass spectrometer (at Southern Methodist University) and a VG-Micromass 602B mass spectrometer (at Scottish Universities Research and Reactor Centre). Values for the relative concentration are given relative to standard mean ocean water (SMOW) in the familiar δ notation (in ‰) in Tables 2 and 3 to a precision of about ±1‰ where

$$\delta D_{\text{sample}} = \left(\frac{(D/H)_{\text{sample}}}{(D/H)_{\text{standard}}} - 1\right) \times 10^3 \qquad (1)$$

and the equilibrium fractionation factor, α^e, is related to δD by

$$\alpha^e_{\text{chl-H}_2\text{O}} = \frac{(D/H)_{\text{chlorite}}}{(D/H)_{\text{water}}} = \frac{1 + (\delta D_{\text{chlorite}}/1000)}{1 + (\delta D_{\text{water}}/1000)}. \qquad (2)$$

INTERPOLATION OF α^e

Complete isotope exchange at any temperature is demonstrated by attainment of the same final fractionation factor (α_f) either in experiments run at the same temperature with starting waters of different isotope composition, or in experiments run with waters of the same isotope composition run for different times ($\alpha_f \neq \alpha_i$, where α_i is the initial mineral-water isotope fractionation factor). For most experiments, hydrogen-isotope exchange between chlorite and water was so slow that equilibrium was not attained, and the interpolation method of Northrop and Clayton (1966), modified by Suzuoki and Epstein (1976), was used to calculate α^e from the relationship

$$(\alpha_i - 1) = (\alpha^e - 1) - A(\alpha_f - \alpha_i), \qquad (3)$$

(where α_f and α_i are the final and initial fractionation factors and A is a constant related to the extent of isotope exchange) for two or more experiments of the same duration run with different starting waters. In practice, α^e may be obtained graphically, algebraically, or by least-squares analysis from the intercept $10^3(\alpha^e - 1)$, in plots of $10^3(\alpha_i - 1)$ vs. $10^3(\alpha_f - \alpha_i)$, where A is the slope of the line fitted through the data for any group of experiments with different starting waters (α_i) at constant T and time. The theoretical kinetic basis of this approach is well founded (Northrop and Clayton, 1966), and the internal consistency of experimental hydrogen-isotope exchange data observed using this partial-exchange interpolation method has been noted in several studies (Suzuoki and Epstein, 1976; Graham et al., 1980, 1984a). The increasing uncertainty of interpolation of α^e at low extents of isotope exchange has been noted by Graham et al. (1980). Uncertainties are discussed in detail below.

Graham et al. (1980) suggested that the interpolation method may not necessarily be applicable to minerals such as chlorite and serpentine that contain hydrogen in more than one site, depending upon the rate-determining mechanism in the exchange reaction. This method was used by Sakai and Tsutsumi (1978) in their experimental study of hydrogen-isotope exchange between serpentine and water, but none of their experiments attained isotopic equilibrium so that independent verification that the interpolated values of $\alpha^e_{\text{serp-H}_2\text{O}}$ are correct, or that the interpolation method is valid, is not possible. In this study we find good agreement between fractionation factors calculated from partial-exchange experiments at 600°C using the interpolation method and determined by isotope equilibrium in longer runs at the same temperature (Table 3). This observation is consistent with—but not conclusive proof of—the validity of the interpolation method for the chlorites, and by inference possibly also for the serpentines.

Applicability of the interpolation method to the chlorites with hydrogen in different structural sites may indicate that the rate-determining step in the process of isotope exchange is related to the transport of hydrogen through the mineral structure (e.g., Graham, 1981), rather than to the breaking and reforming of O–H bonds.

RESULTS

Results of valid experiments on hydrogen-isotope exchange between chlorite and water are given in Table 3, together with final fractionation factors (α_f) and interpolated equilibrium fractionation factors (α^e). Discussion of these results necessitates (1) a consideration of the experimental problems of hydrogen diffusion through capsule walls and hydrogen-isotope exchange between capsule contents and the external experimental environment and (2) a consideration of the uncertainties arising from this source and from analytical uncertainties, in order that the validity of any experiment may be assessed and realistic constraints placed upon the uncertainty in α^e.

Hydrogen-isotope exchange between capsules and pressure medium

Hydrogen diffusion through capsule walls and D-H exchange between capsules and pressure medium during high *P-T* gas-media experiments may cause significant shifts in the bulk δD of experimental charges. These changes in δD in experiments where complete exchange was not attained may seriously limit the precision with which equilibrium fractionation factors may be constrained by the interpolation method, and necessitate a consideration of the mechanisms and relative rates of hydrogen-isotope exchange between mineral and water and between the mineral-water system and the external experimental environment (pressure medium, pressure vessel, furnace, etc.).

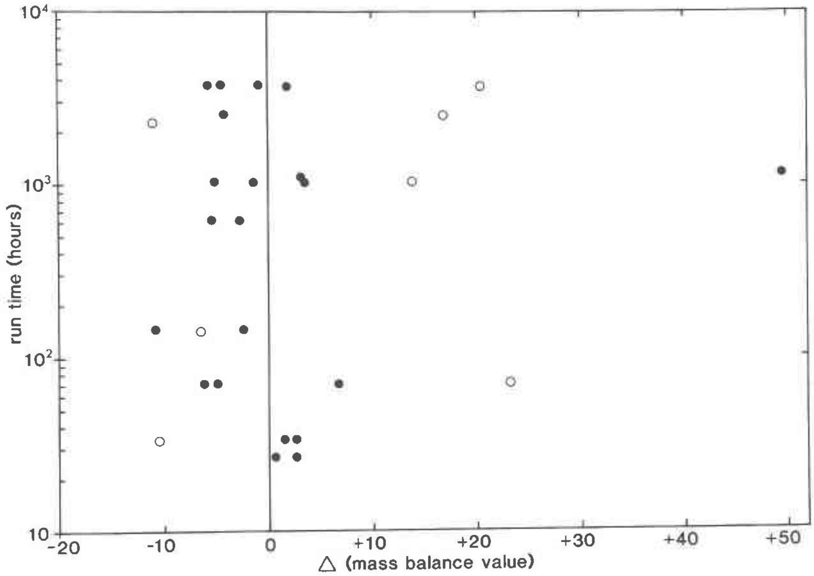

Fig. 1. Plot of mass-balance value (Δ) against run time (hours) to illustrate shifts in bulk δD of chlorite-water hydrogen-isotope exchange experiments. Δ values calculated using Eq. 5. Filled circles indicate runs listed in Table 3. Open circles indicate runs rejected on basis of anomalous hydrogen yields or inconsistent kinetics. See discussion in text.

Graham et al. (1980) suggested that changes in δD of experimental charges could be minimized at temperatures below about 650°C by use of thick-walled (0.5 mm) Au capsules. However, the results of hydrogen-isotope exchange experiments between amphibole and water (Graham et al., 1984a) indicated that Fe-rich amphibole charges underwent significant shifts in δD at temperatures less than 650°C owing to oxy-hornblende reactions driven by the buffering effect of bomb walls on the charges, while Fe-poor charges showed little or no significant change in δD in experiments up to 850°C. Also, experiments in internally heated gas vessels were found to be much less susceptible to change in bulk δD than those in Nimonic cold-seal pressure vessels (Graham et al., 1984a, Table 3). In all these studies (see also Graham et al., 1980, App. I), changes in bulk δD of charges were always in the direction of *D enrichment*.

Mass-balance calculations for isotope exchange experiments in this study were calculated from the relationship

$$x\delta D^{i}_{chl} + y\delta D^{i}_{H_2O} = x\delta D^{f}_{chl} + y\delta D^{f}_{H_2O}, \qquad (4)$$

where x is the number of moles of H in chlorite and y is the number of moles of H in the water and i and f refer to hydrogen-isotope compositions before and after experiments, respectively. From Equation 4, mass-balance values were calculated as

$$\Delta = (x\delta D^{f}_{chl} + y\delta D^{f}_{H_2O}) - (x\delta D^{i}_{chl} + y\delta D^{i}_{H_2O}). \qquad (5)$$

Δ values for all experiments are plotted against run time in Figure 1. Clearly, numerous runs suffered significant changes in δD down to temperatures as low as 400°C, despite the absence of significant Fe in the chlorite and despite the use of thick-walled Au capsules, which clearly did not inhibit D-H exchange between charge and pressure medium. In addition, unlike previous experimental hydrogen-isotope studies in the high-pressure laboratories at Edinburgh, significant changes in bulk δD were in the direction of *both* D enrichment and D depletion in experiments in both cold-seal and internally heated pressure vessels (Fig. 1). In addition to hydrogen diffusion through capsule walls during high *P-T* experiments, shifts in bulk δD of charges may result from gain of atmospheric moisture or loss of water during loading and welding of capsules, analytical error, and incomplete removal of free water from quenched capsules or of structural water from chlorite. These several alternative sources of error may often be identified by yields of hydrogen that are inconsistent with starting water or chlorite contents. Indeed, some runs showing large δD shifts in Figure 1 gave anomalous hydrogen yields. However, numerous runs giving satisfactory hydrogen yields showed shifts in δD that exceed reasonable isotopic analytical error.

The related problems of controlling the δD of charges during high *P-T* hydrogen-isotope exchange experiments and of interpreting and understanding the mechanisms and processes causing δD shifts have been discussed by Graham et al. (1980, 1984a) and recently by Richet et al. (1986). Whatever the sources of hydrogen in the Ar pressure medium in these studies (bomb walls, filler rods, moisture from furnace cement or atmospheric sources, impurities in bottle Ar, etc.), tentative explanations to date have focused on the existence of large f_{H_2} gradients across capsule walls (Graham et al., 1980; Richet et al., 1986). A detailed discussion of these processes and of the conclusions of Richet et al. (1986) will be presented elsewhere. However, here we make the following observations and conclusions regarding δD shifts from experimental data of this and previous studies (cited above): (1) The occurrence of both D enrichment and D depletion during chlorite-water exchange experiments in both internally heated and cold-seal pressure vessels (Table 3) negates the suggestion of Richet et al. (1986) that the pressure medium in the internally heated pressure vessels in their D-H exchange on melt-vapor systems was much more reducing than in our exchange experiments. (2) We note that Δ in Figure 1 shows no time dependence. (3) We note that the data on diffusivity of protium and deuterium through Pt (Ebisuzaki et al., 1968), if applicable to other metals of comparable structure such as Au, would cause the rapid elimination of initial, transient f_{H_2} gradients between capsules and pressure media well within the time scale of our shortest exchange experiments. This latter conclusion is quite consistent with the observed absence of a time dependence for Δ in our runs. Therefore we believe that our chlorite + H_2O charges approach a situation of hydrogen-isotope *exchange equilibrium* with hydrogen-bearing contaminants of widely variable D/H in the pressure medium well within the time scale of our shortest experiments. Apparent absence of δD shifts in any experiment may be due to coincidental similarity of δD in charge and pressure medium.

The rate of this capsule–pressure medium exchange process is much faster than the rate of exchange of hydrogen isotopes between chlorite and water in this study, as is evident from an analysis of the kinetics of the latter exchange (Table 3; see discussion below). Therefore, a first-order correction to the experimental data for the effects of changing bulk δD during high *P-T* experiments may be made by assuming that the entire shift in δD, calculated as Δ (the mass-balance values derived from Eq. 5 and listed in Table 3), may be attributed to a shift in $\delta D^i_{H_2O}$ (the δD of the starting water) *before* significant exchange between chlorite and water has been achieved. Accordingly, in experiments in which 100% exchange between chlorite and water has not been attained, modified values of $\delta D^i_{H_2O}$ ($\delta D'^i_{H_2O} = \delta D^i_{H_2O} - \Delta$) have been used to calculate the effective initial chlorite-water fractionation factor (α'_i) used in interpolating the equilibrium fractionation factors (Table 3). It is interesting to note that the equilibrium factors thus interpolated are, with one exception (runs 26 and 27), within 5–6‰ of the interpolated values of $10^3 \ln \alpha^e$ calculated using uncorrected values of α_i from Table 2.

Partial-exchange experiments listed in Table 3 and used to interpolate equilibrium fractionation factors have mass-balance values (Δ) up to over 10 (positive or negative). Many experiments with Δ values greater than ±11, and a few with smaller Δ values, gave anomalous hydrogen yields for water or chlorite and were rejected. Beyond this, internal consistency of results is taken as a primary criterion of data validity; kinetic analysis of the experimental data in Table 3 provides a useful approach to demonstrating such internal consistency (Graham, 1981) and is considered below (Fig. 5).

Consideration of errors and uncertainties

A rigorous quantitative treatment of uncertainties in the experimental and analytical data is problematical, as is calculation of realistic uncertainties in the equilibrium fractionation factors. Several steps are involved in the derivation of each valid datum, each with some attached uncertainty or error. Some sources of uncertainty (e.g., analytical error in hydrogen-isotope analysis) are normally distributed, whereas others (shifts in δD of charges by exchange with the pressure medium) are not. Correction of the experimental data for the latter effect has been considered in detail above. The analytical uncertainty, estimated to be ±1‰, is the most tractable, and probably the largest, source of normally distributed uncertainty. This ±1‰ uncertainty gives rise to an uncertainty of ±1.41‰ in $10^3 \ln \alpha_f$ ($\approx \delta D^f_{chl} - \delta D^f_{H_2O}$) for any chlorite-water pair. This will be the uncertainty in $10^3 \ln \alpha^e$ only when complete exchange is attained (e.g., runs 2 and 3, Table 3). However, it is evident from a consideration of the graphical representation of the interpolation method for deriving equilibrium fractionation factors from partial-exchange experiments (e.g., Northrop and Clayton, 1966; Suzuoki and Epstein, 1976) that the uncertainty in $10^3 \ln \alpha^e$ will be greater than ±1.41 and will increase with decreasing extent of exchange (*f* in Table 3). Taking limiting values of δD for chlorite and water consistent with analytical uncertainty in each run used to interpolate values of α^e, uncertainties in interpolated values of equilibrium fractionation factors ($10^3 \ln \alpha^e$) were calculated (Table 3), ranging from ±1.7 at 80% exchange (runs 22 and 23) to ±3.7 at 38% exchange (runs 26 and 27).

Relationship between fractionation factor (α^e) and temperature

Exchange rates (given by the extent of exchange, *f* in Table 3) in the system chlorite-H_2O were sufficiently slow that complete exchange ($f = 1$) was attained in only one pair of experiments, run at 600°C for 46 d with the fine-grained starting material; although both charges (runs 2 and 3 in Table 3) gained D, attainment of 100% exchange, as demonstrated by the same value of α_f, obviates the need for interpolation of α^e. Runs 16 and 17 with the medium-grained starting material at 600°C for only 71 h, attained only 52% exchange, but the interpolation method gave a value of α^e comparable within experimental error. These results would seem to justify the application of the interpolation method to the chlorites, as discussed above.

Owing to slow exchange and decreasing extent of exchange (*f*), interpolated values of α^e are less well constrained at lower temperature, despite the long run times. Thus at 500°C, runs attained only 38–47% exchange (26–43 d). At 300 and 400°C, exchange was insufficient to constrain interpolated values of α^e (Table 3).

Equilibrium fractionation factors at 700, 600, and 500°C are given in Table 3 and plotted in Figure 2. At 700 and 600°C, where there is 50–100% exchange, equilibrium

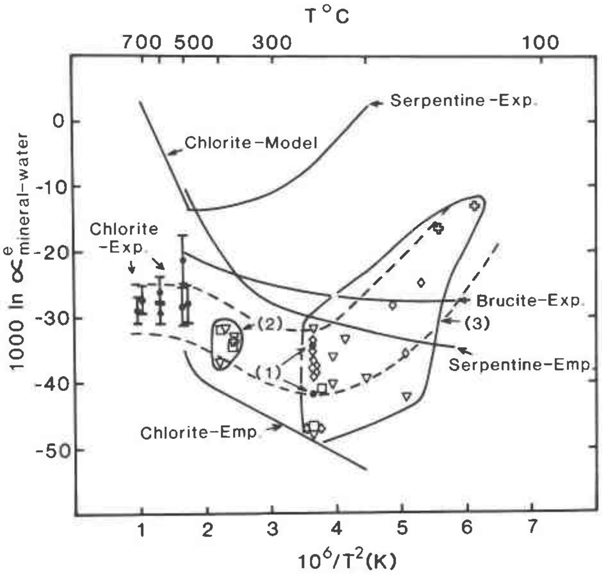

Fig. 2. Relationships between hydrogen-isotope fractionation factor (1000 ln $\alpha^{e}_{\text{mineral-water}}$) and temperature [plotted as $10^6/T^2$ (K)] for minerals in the system MgO-FeO-Al_2O_3-SiO_2-H_2O. Chlorite-Exp.: this study; Chlorite-Model: calculated for clinochlore composition using the model of Suzuoki and Epstein (1976) (see text). Chlorite-Emp: empirical curve of Taylor (1974); Brucite-Exp.: experimental data of Satake and Matsuo (1984); Serpentine-Exp.: experimental data of Sakai and Tsutsumi (1978); Serpentine-Emp.: empirical curve of Wenner and Taylor (1973). Tentative extrapolations (dashed lines) of experimental data (this study) for chlorite-H_2O based on fractionation factors given in Table 4 and derived from (1) Kuroda et al. (1976); (2) Heaton and Sheppard (1977); (3) Marumo et al. (1980). Symbols for varying Fe/(Fe + Mg) in chlorite: filled circle = 0 to 0.09; cross = 0.20 to 0.29; diamond = 0.30 to 0.39; triangle = 0.40 to 0.49; square = 0.50 to 0.69. See also Marumo et al. (1980, Fig. 8).

fractionation factors derived from different pairs of runs at each temperature are in reasonable agreement. At 500°C, equilibrium fractionation factors calculated from runs using the fine- and medium-grained starting materials ($0.4 < f < 0.5$) are in close agreement ($10^3\ln \alpha^e \approx -28$), but are significantly more negative than those calculated from runs using the coarse-grained starting material ($10^3\ln \alpha^e \approx -21$; $f = 0.38$). We place more reliance on the runs with the higher extents of exchange and consider −28 to be the best estimate of the chlorite-water fractionation at 500°C. There is no evidence in all these data for any measurable temperature dependence for the chlorite-water hydrogen-isotope fractionation over the temperature range 500–700°C, the fractionation factor remaining close to $10^3\ln \alpha^e = -28$.

Discussion

Controls on fractionation factors

Suzuoki and Epstein (1976) proposed a general relationship between hydrogen-isotope fractionation factor and octahedral cation composition (Mg:Fe:Al) applicable to sheet silicates, in which $1000 \ln \alpha^{e}_{\text{mineral-}H_2O} = -22.4(10^6/T^2) + (2X_{Al} - 4X_{Mg} - 68X_{Fe}) + 28.2$, where X_M is the mole fraction of cation M in octahedral sites, but predicted that chlorite might be deuterium depleted relative to fractionation factors predicted by the model because of hydrogen bonding in chlorite. Comparison of model versus experimentally measured fractionation factors for the chlorite used in this study shows this to be the case (Fig. 2), the experimentally measured fractionation factors being 15 to 30‰ more negative than predicted by the model of Suzuoki and Epstein (1976).

The effect of hydrogen bonding on D-H fractionation in mineral-water systems was studied in detail by Graham et al. (1980), who confirmed the prediction of Suzuoki and Epstein (1976) that hydrogen-bonded minerals should strongly concentrate protium relative to non–hydrogen-bonded minerals. A qualitative model relating hydrogen-bond structure and geometry to fractionation factor and exchange rate (Graham et al., 1980) was subsequently shown not to be supported by more recent neutron-diffraction studies of hydrogen in epidote.

Recent studies of the chlorite structure show that hydroxyls occupy two structurally different sites in the brucite and talc layers. The structure permits hydrogen bonding between hydroxyls of the brucite layer and oxygens of the talc layer, whereas hydrogens within the talc layer are not hydrogen bonded (Phillips et al., 1980; Joswig et al., 1980). Long hydrogen bonds between the brucite and talc layers stabilize the chlorite structure and contribute significantly to the interlayer bond energy (Bish and Giese, 1981). Therefore, we might expect the hydrogen-bonded hydroxyls associated with the brucite layer to concentrate protium relative to the talc layer; that is, hydrogen isotopes will fractionate differently between the brucite layer and water than between the talc layer and water. Dehydration of chlorites occurs in two stages, with dehydration of the brucite layer occurring at lower temperatures than dehydration of the talc layer, and isotopic analysis of water released during step-heating of natural chlorite shows that water in the brucite layer is lower in δD than water in the talc layer (Suzuoki and Epstein, 1976), as would be expected if hydrogen associated with the brucite layer in chlorite is hydrogen bonded.

The experimentally determined chlorite-water fractionations (Fig. 2) are significantly more negative than fractionations in the systems brucite-water (Satake and Matsuo, 1984) and serpentine-water (Sakai and Tsutsumi, 1978), reflecting the hydrogen bonding in chlorite that is absent in brucite and serpentine (Suzuoki and Epstein, 1976; Satake and Matsuo, 1984). Comparison of the chlorite-water and brucite-water curves (Fig. 2) is also complicated by the distribution of Al in chlorites, which is strongly partitioned into the brucite layer (Phillips et al., 1980; Joswig et al., 1980), such that in the chlorite used in this study, between one-third and one-half of the brucite-layer octahedra are occupied by Al.

TABLE 4. Chlorite-water fractionation factors estimated from chlorite D/H analyses

T (°C)	$10^3 \ln \alpha^e_{\text{chl-water}}$	Chlorite Fe/(Fe + Mg)
From Kuroda et al. (1976)		
200–300	−42.1	0.06
200–300	−34.7	0.07
From Heaton and Sheppard (1977)		
400	−31.7	0.51
400	−31.7	0.42
400	−36.9	0.48
370	−32.8	0.40
370	−34.8	0.63
370	−33.8	0.28
From Marumo et al. (1980)		
130	−13.3	0.28
140	−16.6	0.23
160	−16.6	0.36
170	−35.8	0.35
170	−42.2	0.43
180	−28.2	0.43
200	−39.1	0.43
220	−33.4	0.43
230	−40.3	0.43
230	−36.0	0.44
240	−40.9	0.51
250	−37.5	0.36
250	−36.4	0.39
250	−37.7	0.36
250	−31.7	0.44
250	−35.3	0.36
250	−33.5	0.35
250	−46.7	0.52
250	−47.8	0.48
250	−37.4	0.34
250	−39.1	0.36

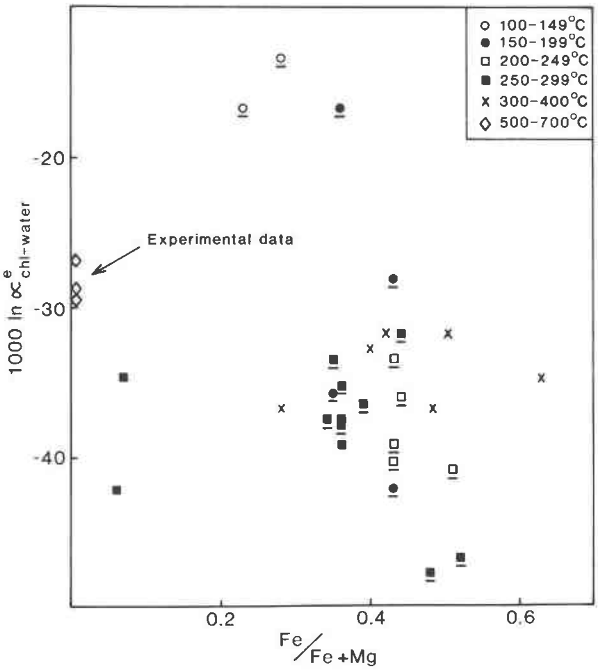

Fig. 3. Plot of hydrogen-isotope fractionation factor (1000 ln $\alpha^e_{\text{chl-water}}$) vs. Fe/(Fe + Mg) (chlorite). Data from this study (experimental data), and Kuroda et al. (1976), Heaton and Sheppard (1977), and Marumo et al. (1980). Empirical data listed in Table 4. Data of Marumo et al. (1980) are underlined.

Comparison with empirical chlorite-water fractionations and effect of Fe/Mg

Taylor (1974) calculated an empirical curve for D-H fractionation in the system chlorite-water (Fig. 2) using data for chlorites from pelitic schists. The compositions and origins of these chlorites are not reported, but it may be surmised that they were comparably or slightly less aluminous than the chlorite used in this study (Velde and Rumble, 1977) but with extensive and variable replacement of Mg by Fe^{2+}. The extrapolation of this curve to higher temperature lies close to the experimentally determined fractionation factors (Fig. 2). On the other hand, a more securely based empirical calibration of chlorite-water hydrogen-isotope fractionation discussed below suggests different fractionation factors from Taylor's calibration while remaining consistent with the experimental data.

A limited amount of data on the D/H of natural chlorites from metamorphic (ocean floor), geothermal, and hydrothermal environments in which temperature, δD of coexisting water, and Fe/Mg (chlorite) are well-known (Kuroda et al., 1976; Heaton and Sheppard, 1977; Marumo et al., 1980) allow us to assess the effects of Fe/Mg and temperature on chlorite-water fractionations over a range of temperatures down to 100°C (Table 4). Although the empirical calibrations must be treated with caution because of uncertainty regarding crystallization temperatures, δD of coexisting water, and continued equilibration of chlorites with water to temperatures well below those of crystallization of chlorite during slow cooling (Graham, 1981), the data in Table 4 represent low-temperature chlorites from geologic situations where cooling rates are relatively fast by geologic standards and δD (H_2O) and temperature are quite well constrained, particularly the geothermal drill-core data of Marumo et al. (1980) in which T and δD (H_2O) may be measured directly.

Marumo et al. (1980) have asserted that there is a correlation between $\alpha_{\text{chl-H}_2\text{O}}$ and Fe/Mg (chlorite), and that $\alpha_{\text{chl-H}_2\text{O}}$ "does not depend on the temperature explicitly." However, the numerically smallest and largest fractionations (1000 ln α) in their data set, on which their supposed Fe/Mg effect is based, are from their lowest- and highest-temperature samples, respectively (Fig. 3). The effects of temperature and Fe/Mg (chlorite) on chlorite-water fractionation cannot be unambiguously separated in the data of Marumo et al. (1980), and, taking the data of Table 4 together with the experimental data (Figs. 2, 3), the above assertion of Marumo et al. is not supported. The data in Table 4 do not include information on the octahedral Al contents of the chlorites, which could also influence chlorite-water D-H fractionations. However, from these data we may construct a tentative and empirical calibration of chlorite-water D-H fractionations for $T < 400$°C that is broadly consistent with the 500–700°C experimental data for Fe-poor aluminous chlorite. These data (Fig. 2) are only sufficient to constrain 1000 ln $\alpha^{e}_{chl\text{-}H_2O}$ to ±5‰ at best at any temperature, but allow us to make the following tentative conclusions: (1) Any Fe/Mg (chlorite) dependence is within the scatter of the data for $0 < Fe/Mg < 0.6$ and must await experimental verification. (2) The experimental data for Fe-poor sheridanite indicate that 1000 ln $\alpha^{e}_{chl\text{-}H_2O}$ is about -28 over the temperature range 500–700°C, with no temperature dependence. (3) Over the temperature range 500–200°C, fractionations show only a small temperature dependence at most, with 1000 ln $\alpha^{e}_{chl\text{-}H_2O}$ becoming more negative with decreasing temperature, but lying in the range -30 to -40. (4) Below 200°C, fractionations may become more positive with decreasing temperature, as found in the experimentally studied systems serpentine-H_2O (Sakai and Tsutsumi, 1978), epidote-H_2O, and boehmite-H_2O (Graham et al., 1980). (5) The empirical calibration in Figure 2 is shifted by 5 to 10‰ to more positive fractionations than those deduced by Taylor (1974) using chlorites from pelitic schists.

Implications for experimental actinolite-H_2O D-H fractionations

Graham et al. (1984a) experimentally determined the D-H fractionation for actinolite-water at 400°C to be 1000 ln $\alpha^{e}_{actinolite\text{-}H_2O} = -29$, using an actinolite from a metamorphosed basaltic rock. In these experiments, 55–60% exchange was attained in 59 d. However, the actinolite starting material contained a small amount of chlorite that could not be separated, and therefore the measured fractionation is only approximate. In this study, much longer experiments (105 and 157 d) produced negligible D-H exchange between chlorite and water at 400°C. Therefore, unless the chlorite intergrown with actinolite has a particularly small *effective* grain size, this chlorite in all probability underwent very limited exchange during the actinolite-water exchange experiments. Therefore, the measured actinolite-water D-H fractionation at 400°C may be a good approximation to the equilibrium fractionation factor.

KINETICS OF D-H EXCHANGE

The kinetics of hydrogen-isotope exchange between chlorite and water may be quantified by application of reaction-kinetics theory (Graham, 1981). Here we assume, following Graham (1981) and Graham et al. (1984a), that exchange reactions may be approximated (empirically) by second-order kinetics, so that

$$f/(1 - f) = K_2 t, \tag{6}$$

where f is the fractional approach to equilibrium (Table 3), t is the time of exchange, and K_2 is the second-order rate constant. Activation energies (Q) for the rate-determining step may be derived from the Arrhenius relationship

$$\log K_2 = \log a - Q/2.303RT, \tag{7}$$

where a is a constant (the pre-exponential factor).

Satake and Matsuo (1984) chose to assume that hydrogen-isotope exchange between brucite and water followed first-order kinetics, although they were unable to demonstrate this unequivocally (cf. Graham, 1981). Second-order kinetics give an equally good linear fit of the brucite data to the Arrhenius relationship as do first-order kinetics. Nonetheless, it is quite likely that the brucite-water experimental data fit a *different* rate law than other experimental OH mineral-water exchange data, because Satake and Matsuo (1984) observed that dissolution-reprecipitation was very likely the major process of D-H exchange rather than volume diffusion of hydrogen in the solid (cf. Graham, 1981).

Minerals may change in grain size during exchange experiments owing to mechanical breakdown or dissolution-reprecipitation; if this occurs, exchange rate may vary with time. Chlorite-water exchange experiments used small amounts of water (cf. Graham et al., 1980) in order to minimize grain dissolution-reprecipitation. Chlorite run products of five exchange experiments were examined by SEM in order to assess the extent of either of these processes. Comparison of run products with starting materials (Fig. 4) indicates that no significant changes in grain size or morphology have occurred and that chlorite D-H exchange must proceed dominantly by volume diffusion of hydrogen in the chlorite.

An Arrhenius plot of second-order constants (log K_2) vs. $10^3/T$ for the chlorite-water exchange data (Fig. 5) gives good and consistent linear fits for the medium and coarse grain-size fractions and is a useful test and demonstration of the internal consistency of the experimental data set. Activation energies for hydrogen transport in chlorite are around 150 kJ (36 kcal)/mol H for the medium and coarse grain sizes (Table 5). Rate constants for the coarse grain size are displaced to more negative values of log K_2 than those for the medium and fine grain sizes (Fig. 5), consistent with the conclusion that the effective chlorite grain size has not varied during exchange experiments, that exchange has proceeded by volume diffusion of hydrogen in chlorite, and that the measured grain sizes are the effective grain sizes for diffusion. Calculated activation energies are much higher than for hydrogen exchange between other hydrous minerals and water (cf. Graham, 1981; Graham et al., 1984a), as would be predicted from the very slow exchange rates at $T \leq 400°C$.

DIFFUSION OF HYDROGEN IN CHLORITE: CLOSURE TEMPERATURES

Calculation of diffusion coefficients

Closure temperatures for cessation of hydrogen-isotope exchange between chlorite and hydrous fluid in cooling metamorphic and hydrothermal systems may be calculated from estimated diffusion parameters for hydrogen diffusion in chlorite. Methods of calculating hydrogen-diffusion coefficients from experimental data on hydrogen-isotope exchange are described in detail by Graham (1981), and their application to the chlorites is briefly outlined here.

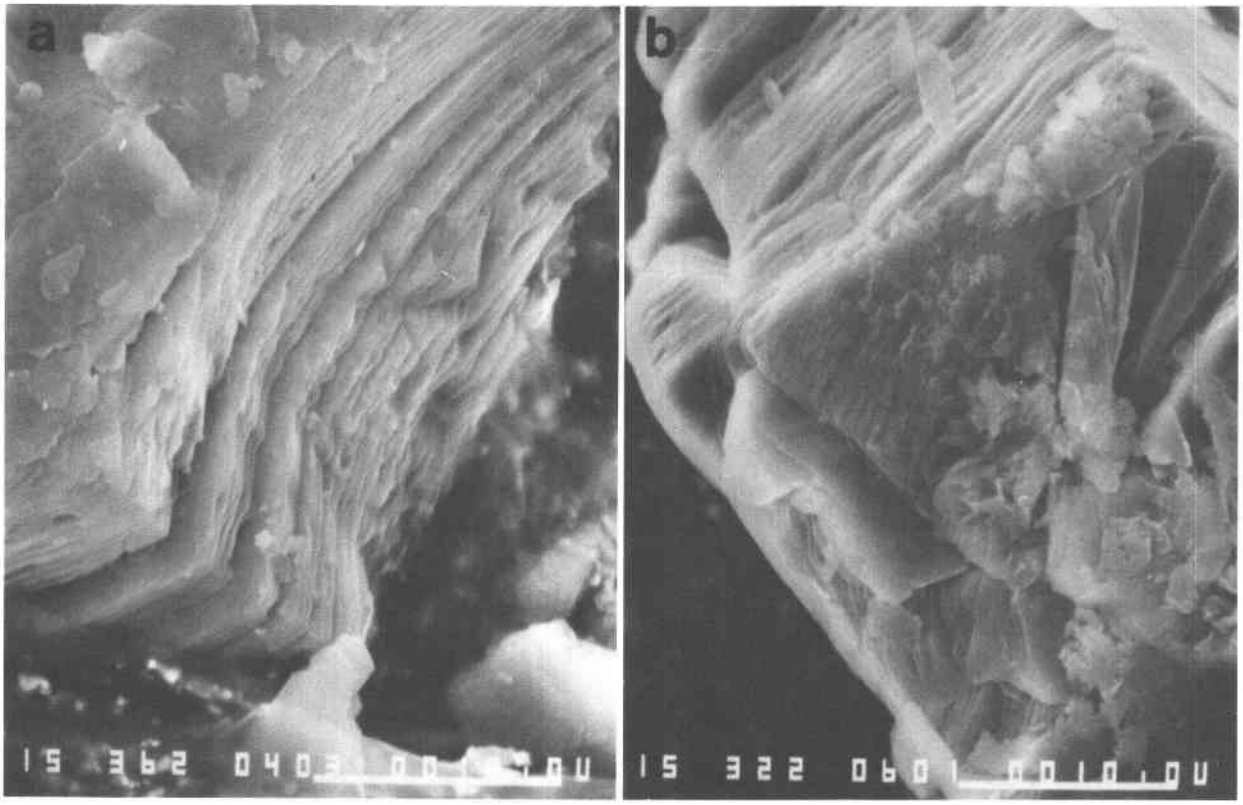

Fig. 4. Scanning electron microscope (SEM) photographs of fine-grained chlorite in starting material (b) and in run product (a) of exchange experiment at 600°C for 217 h. Scale bar is in micrometers. Photographs indicate absence of solution-reprecipitation or mechanical breakdown during exchange experiments.

The calculation of diffusivities involves a knowledge of grain geometries in order to account for diffusional anisotropies, especially for minerals with well-developed cleavages such as the sheet silicates. The mean effective grain diameters, plate thicknesses, and aspect ratios for the three chlorite grain-size fractions were measured optically and are given in Table 6. SEM observations showed that measured grain thicknesses were greater than true thicknesses owing to the difficulty of viewing the platy grains edge-on in optical mounts, and grain thicknesses have been adjusted accordingly to half the optically estimated thicknesses to take account of this problem and to assess the effect on calculated diffusion coefficients of varying the grain thickness. Two geometrical models are applicable to hydrogen diffusion in platy minerals: (1) the infinite cylinder model in which hydrogen diffuses parallel to the layers and (2) the infinite plate model in which hydrogen diffuses perpendicular to the layers. For a stirred solution of limited volume, Equations 5.36 and 4.43 respectively of Crank (1975) are applicable (see Graham, 1981). Corresponding values of log D calculated using these equations are given in Table 3. For the plate model, both measured and adjusted plate thicknesses were used; the effect of reducing plate thickness by half is to reduce D by about half an order of magnitude.

The correct diffusion model should yield similar diffusion coefficients for the different grain sizes at any temperature. However, although chlorite is a platy mineral, the aspect ratios of the starting materials are not large enough to allow a clear-cut choice to be made between the two models (cf. muscovite; Giletti and Anderson, 1975; Graham, 1981), because for both models all data, irrespective of grain size, may be fitted to a single linear regression on an Arrhenius plot (Fig. 5), with a correlation coefficient (r^2) better than 0.97 (Table 5). Although the data may be interpreted to mean that hydrogen diffusion occurs at comparable rates parallel and perpendicular to the layers, it is more likely, by analogy with muscovite (Graham, 1981) that hydrogen diffusion will occur faster parallel to the layers (cylinder model). For this case, diffusivities are one to two orders of magnitude faster than for the plate model (depending on the adopted plate thickness).

Calculated activation energies for both models are comparable at 172 kJ (41 kcal)/mol H and 167 kJ (40 kcal)/mol H for cylinder and plate models, respectively (Table 5). These activation energies are of considerable interest, being significantly the largest for any hydrous mineral studied to date. By comparison the activation energies for hydrogen diffusion in muscovite, hornblende, tremolite, and zoisite are 121 (29), 84 (20), 71 (17), and 103 (24.5) kJ (kcal)/mol H, respectively (cylinder model; Graham, 1981; Graham et al., 1984a) (Fig. 5). It is possible that the large interlayer site in muscovite, for ex-

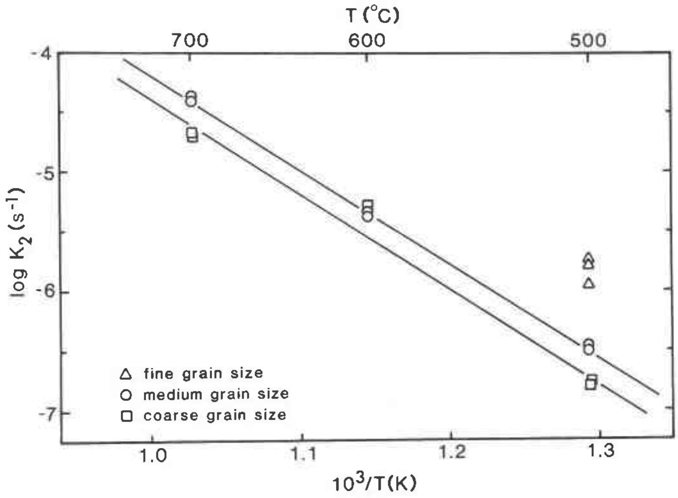

Fig. 5a. Arrhenius plot of second-order rate constants (log K_2) vs. reciprocal temperature for hydrogen-isotope exchange experiments between chlorite and water. Data given in Table 3. See text for discussion.

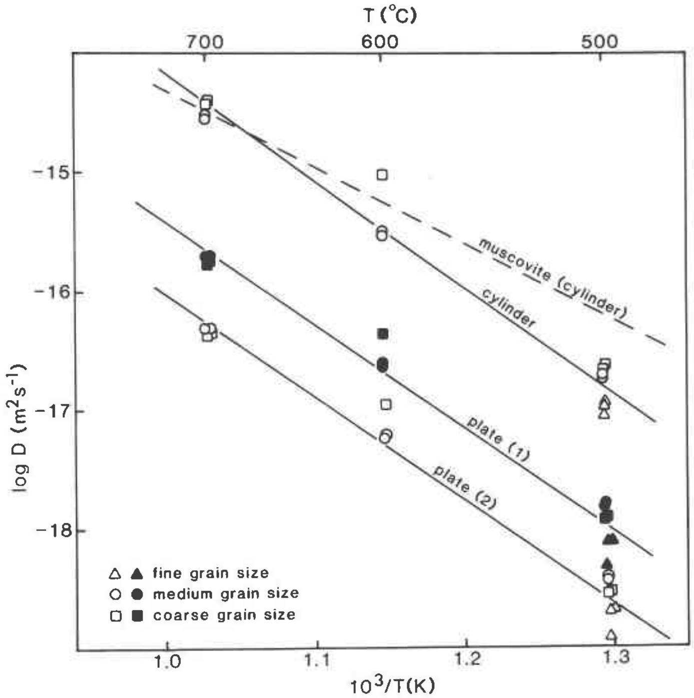

Fig. 5b. Arrhenius plot of diffusion coefficients vs. reciprocal temperature for diffusion of hydrogen in chlorite, using both cylinder and plate models. Plate (1) refers to optically estimated grain thicknesses; plate (2) refers to adjusted grain thicknesses (see Table 6). Muscovite data (cylinder model) from Graham (1981) shown for comparison. Symbols as in Fig. 5(a). Data given in Table 3. See text for discussion.

ample, allows faster transport pathways parallel to the layers than are available in chlorite, where interlayer sites are lacking. Diffusion coefficients for hydrogen diffusion in chlorite, adopting the cylinder model for comparison, are up to 3 to 4 orders of magnitude slower over the range of temperatures of crystallization and cooling of metamorphic and hydrothermal rocks than diffusion coefficients for hydrogen diffusion in other hydrous minerals, excluding epidote (Graham, 1981; Graham et al., 1984a). The implications of these results for calculated closure temperatures for the cessation of hydrogen diffusion in chlorites relative to other hydrous minerals are considered below.

Exchange mechanisms

Matthews et al. (1983) conducted one oxygen-isotope exchange experiment using clinochlore and water at 500°C for 3 d. This experiment achieved only 11% exchange. By comparison, the medium-grained chlorite used in this study attained 45% exchange of hydrogen isotopes at 500°C in 26 d. The grain size of the starting material in the oxygen-isotope exchange study was not stated by

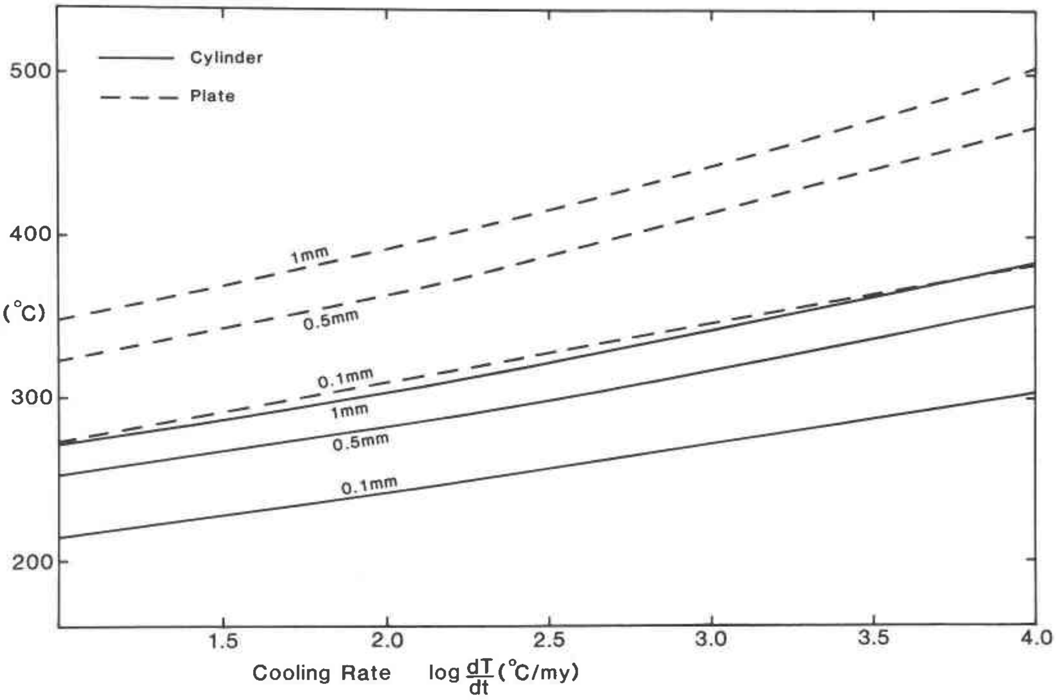

Fig. 6. Plot of calculated closure (blocking) temperature (T_c) vs. logarithm of cooling rate dT/dt (deg/m.y.) for cessation of hydrogen-isotope exchange between chlorite and water, using both plate and cylinder models. Grain sizes (in mm) refer to diameter of chlorite grain (cylinder model) or thickness of chlorite plate (plate model). Calculation method described in text.

Matthews et al. (1983), but was most likely very much finer grained than the chlorite used in this study (Matthews, pers. comm.), indicating that hydrogen diffusion in chlorites is more rapid than oxygen diffusion. This is consistent with the observed absence of solution-reprecipitation in our experiments and with the observations of Graham (1981) that hydrogen diffusion in muscovite proceeded fastest parallel to the layers and was about five orders of magnitude faster than oxygen diffusion, which occurred fastest perpendicular to the layers (Giletti and Anderson, 1975). Similarly, O'Neil and Kharaka (1976) observed negligible oxygen-isotope exchange between clay minerals and water in low-temperature (≤350°C) exchange experiments in which significant hydrogen-isotope exchange occurred. These authors concluded that hydrogen and oxygen isotopes exchanged by different mechanisms in the absence of solution-reprecipitation.

TABLE 5. Activation energies (Q) derived from the Arrhenius relationship

	a	b	Q (kJ/mol)	Q (kcal)	r^2
Chlorite-water hydrogen-isotope exchange at 500–700°C*					
Medium grain size	3.70	−7.89	151.1	36.1	0.99
Coarse grain size	3.56	−7.95	152.2	36.4	0.99
Hydrogen diffusion in chlorite at 500–700°C**					
Cylinder model	−5.21	−8.97	171.7	41.0	0.97
Plate model (measured thickness)	−6.70	−8.72	166.9	39.9	0.98
Plate model (adjusted thickness)	−7.32	−8.70	166.5	39.8	0.98

Note: $b = Q/2.303R$; r_2 is the correlation coefficient; T is in kelvins.

* Q calculated by least-squares fitting of calculated second-order rate constants (K_2) to the equation $\log K_2 = a + b(10^3/T)$. Grain geometries are given in Table 6.

** Q calculated for both the infinite-cylinder and plate models by least-squares fitting of calculated diffusion coefficients to the equation $\log D = a + b(10^3/T)$.

Closure temperatures

Assuming that the diffusion coefficients for hydrogen diffusion in chlorite determined at 500–700°C in this study may be extrapolated to lower temperatures (i.e., that diffusion mechanisms are not temperature dependent), clo-

TABLE 6. Chlorite grain geometries

	Coarse	Medium	Fine
Nominal grain size (μm)	63–105	44–63	<44
Average grain diameter (μm)	167.6	109.9	34.5
Measured grain thickness (μm)	20.6	16.7	5.0
Adjusted grain thickness (μm)	10.3	8.4	2.5
Aspect ratio	16.3	13.1	13.8

Note: Average grain diameters and thicknesses measured optically. Measured grain thicknesses are too large due to difficulty of viewing platy grains edge-on. Grain thicknesses were adjusted to half the measured values, and both sets of thicknesses were used in diffusion-coefficient calculations to assess the effect of varying grain thickness.

sure temperatures for the cessation of hydrogen-isotope exchange between chlorite and water during cooling of metamorphic or hydrothermal rocks may be modeled as a function of grain size and cooling rates. The closure temperatures (T_c) were calculated using the relationship

$$T_c = \frac{Q/R}{\ln\left[\dfrac{-ART_c^2(D_0/a^2)}{Q(dT/dt)}\right]} \quad (8)$$

after Dodson (1973, Eq. 23), which is readily solved by iterating values of T_c; Q is the activation energy for diffusion of hydrogen in chlorite (Table 5), A is the diffusional anisotropy parameter (= 27 for cylinder; = 8.65 plate), R is the gas constant (= 8.314 $J \cdot mol^{-1} \cdot deg^{-1}$), D_0 is the pre-exponential factor in the Arrhenius relationship, a is the grain-size term (radius of cylinder, half-thickness of plate), and dT/dt is the cooling rate ($deg \cdot s^{-1}$), where cooling rate is assumed to be linear with $1/T$ near T_c. Calculated closure temperatures will show small variations with varying fluid/mineral ratio, as noted by Cole et al. (1983) for experimental oxygen exchange data (e.g., for cylinder model, 10–20 deg variation for two orders of magnitude variation in water-chlorite ratio), but incorporation of this factor into the calculation of T_c requires a more elaborate analysis than has been attempted to date. Figure 6 shows the calculated relationship between T_c and cooling rate for various chlorite grain sizes, for both plate and cylinder models.

The following general conclusions may be drawn from Figure 6. First, in slow-cooling geologic environments such as those of regional metamorphism [e.g., $1 < \log(dT/dt) < 2$], even the largest chlorite crystals in metamorphic rocks will be susceptible to continued hydrogen-isotope exchange with coexisting hydrous fluid to temperatures below those of greenschist-facies metamorphism. Loss of hydrous fluid will of course permit the chlorite to preserve a record of higher-temperature fluid interactions during slow cooling (e.g., Graham, 1981).

The much faster cooling rates likely to characterize hydrothermal greenschist metamorphism of the oceanic crust or contact metamorphism of mafic rocks may be sufficient to lead to closure temperatures for cessation of hydrogen-isotope exchange between chlorite and water that are within the greenschist facies and not far removed from temperatures of chlorite crystallization. This conclusion will, however, be dependent on chlorite grain size and on the diffusion model adopted (Fig. 6).

Finally, computed closure temperatures for chlorites are significantly higher than those for other hydrous minerals (cf. Graham, 1981; Graham et al., 1984a), as would be expected from the high activation energies for hydrogen diffusion in chlorites (Fig. 5). The variations in closure temperatures and activation energies among different hydrous minerals will mean that mineral-mineral hydrogen-isotope equilibrium is unlikely to be preserved if a hydrogen-bearing fluid is present even in small amounts during slow cooling (see also Graham, 1981); preservation of hydrogen-isotope equilibrium, on the other hand, might indicate loss of such a fluid at an early stage of the cooling process.

PETROLOGIC APPLICATIONS

Metamorphism of basic rocks to chloritic "greenstones" in the oceanic crust is thought to have occurred in environments dominated by relatively high fluid/rock ratios, with fast cooling rates being indicated by the very young ages of many studied samples (e.g., Stakes and O'Neil, 1982). For these circumstances, closure temperatures for cessation of hydrogen-isotope exchange between chlorite and water are in excess of 250°C (Fig. 6). Hydrogen-isotope fractionation factors between chlorite and water at temperatures above 250°C should lie in the approximate range $1000 \ln \alpha^{e}_{\text{chl-water}} = -30$ to $-40‰$ (Fig. 2). Inasmuch as chlorite is a major reservoir of hydrogen in the oceanic crust, the above fractionation factor should represent a dominant component of the overall seawater-hydrated oceanic crust hydrogen-isotope fractionation for that portion of Earth's history during which sea-floor spreading has operated.

There are currently limited data available on the δD of chlorites from ocean-floor, metamorphic, or hydrothermal-geothermal environments. Some of these data (Kuroda et al., 1976; Marumo et al., 1980; Heaton and Sheppard, 1977) have been utilized and discussed above in assessing the effect of Fe/Mg on chlorite-H_2O D-H fractionation and the fractionation factors at low temperatures.

Surprisingly few data are available on the δD of chlorite in hydrated mafic rocks of the ocean crust and of ophiolitic rocks. Satake and Matsuda (1979) analyzed the whole-rock δD of hydrated metabasalt from the Mid-Atlantic Ridge in which chlorite (typically 24 modal percent) is the dominant hydrous mineral, and therefore $\delta D_{WR} \approx \delta D_{chl} = -38$ to $-30‰$. Separated chlorites from Mid-Atlantic Ridge greenstones ($-31‰$, $-34‰$; Stakes and O'Neil, 1982) lie within this range of values. At the likely closure temperatures for cessation of D-H exchange during cooling of hydrated ocean crust, water in equilibrium with these rocks should be close to $\delta D_{H_0} = 0‰$ (using fractionation factors estimated from Fig. 2), consistent with a seawater origin.

Similarly, little data exist on the δD of chlorites and coexisting hydrous minerals in metamorphic rocks. Rye et al. (1976) studied the stable isotope composition of coexisting hydrous minerals in high-pressure metamorphic rocks of Naxos (Greece). In a low-grade schist crystallized at about 480°C, chlorite of $\delta D = -55‰$ coexists with white mica, consistent with available experimental and empirical fractionation data (this study; Suzuoki and Epstein, 1976), and the calculated δD_{H_2O} for the metamorphic water is in the range -25 to $-15‰$.

Magaritz and Taylor (1976) reported δD_{chl} and δD_{WR} for chlorite-rich samples in a wide range of metamorphic rocks of the Franciscan Formation of California. Except for samples for the vicinity of the San Luis Obispo ophiolite (see discussion in Sheppard, 1980), chlorites give calculated δD_{H_2O} for metamorphic fluids within the range -36 to -3‰. These estimates are compatible with δD_{H_2O} of metamorphic pore fluids calculated by Magaritz and Taylor (1976).

ACKNOWLEDGMENTS

This work was supported by NATO Grant 0551/82 (to C.M.G. and R.S.H.) and NSF Grant EAR 82-18380 (to R.S.H.). The Experimental Petrology Unit in Edinburgh and isotope geology facilities at the Scottish Universities Research and Reactor Centre are supported by NERC. Discussions with Simon Sheppard, Alan Matthews, and Gawen Jenkin and helpful reviews from John Valley and J. Rice are acknowledged.

REFERENCES

Bish, D.L., and Giese, R.F. (1981) Interlayer bonding in IIb chlorite. American Mineralogist, 66, 1216–1220.

Cole, D.R., Ohmoto, H., and Lasaga, A.C. (1983) Isotopic exchange in mineral-fluid systems. I. Theoretical evaluation of oxygen isotopic exchange accompanying surface reactions and diffusion. Geochimica et Cosmochimica Acta, 47, 1681–1693.

Crank, J. (1975) The mathematics of diffusion. Oxford University Press, London.

Dodson, M.H. (1973) Closure temperature in cooling geochronological and petrological systems. Contributions to Mineralogy and Petrology, 40, 259–274.

Ebisuzaki, Y., Kass, W.J., and O'Keeffe, M. (1968) Solubility and diffusion of hydrogen and deuterium in platinum. Journal of Chemical Physics, 49, 3329–3332.

Giletti, B.J., and Anderson, T.F. (1975) Studies in diffusion, II: Oxygen in phlogopitic mica. Earth and Planetary Science Letters, 28, 225–233.

Graham, C.M. (1981) Experimental hydrogen isotope studies III: Diffusion of hydrogen in hydrous minerals, and stable isotope exhange in metamorphic rocks. Contributions to Mineralogy and Petrology, 76, 216–228.

Graham, C.M., Sheppard, S.M.F., and Heaton, T.H.E. (1980) Experimental hydrogen isotope fractionation factors in the systems epidote-H_2O, zoisite-H_2O and AlO(OH)-H_2O. Geochimica et Cosmochimica Acta, 44, 353–364.

Graham, C.M., Harmon, R.S., and Sheppard, S.M.F. (1984a) Experimental hydrogen isotope studies: Hydrogen isotope exchange between amphibole and water. American Mineralogist, 69, 128–138.

Graham, C.M., Atkinson, J., and Harmon, R.S. (1984b) Hydrogen isotope fractionation in the system chlorite-water. Progress in Experimental Petrology, 6, 139–140. Natural Environment Research Council of U.K. Publication Series D, 25, London.

Heaton, T.H.E., and Sheppard, S.M.F. (1977) Hydrogen and oxygen isotope evidence for seawater-hydrothermal alteration and ore deposition, Troodos Complex, Cyprus. In Volcanic processes in ore genesis, p. 42–57. Institution of Mining and Metallurgy and Geological Society, London.

Jones, A.A. (1981) Charges on the surfaces of the chlorites. Clay Minerals, 16, 347–359.

Joswig, W., Fuess, H., Rothbauer, R., Takéuchi, Y., and Mason, S.A. (1980) A neutron diffraction study of a one-layer triclinic chlorite (penninite). American Mineralogist, 65, 349–352.

Kuroda, Y., Suzuoki, T., Matsuo, S., and Shirozu, H. (1976) A preliminary study of D/H ratios of chlorites. Contributions to Mineralogy and Petrology, 57, 223–225.

Magaritz, M., and Taylor, H.P. (1976) Oxygen, hydrogen and carbon isotope studies of the Franciscan Formation, Coast Ranges, California. Geochimica et Cosmochimica Acta, 40, 215–234.

Marumo, K., Nagasawa, K., and Kuroda, Y. (1980) Mineralogy and hydrogen isotope geochemistry of clay minerals in the Ohnuma geothermal area, northeastern Japan. Earth and Planetary Science Letters, 47, 255–262.

Matthews, A., Goldsmith, J.R., and Clayton, R.N. (1983) Oxygen isotope fractionation between zoisite and water. Geochimica et Cosmochimica Acta, 47, 645–654.

Northrop, D.A., and Clayton, R.N. (1966) Oxygen isotope fractionation in systems containing dolomite. Journal of Geology, 74, 174–176.

O'Neil, J.R., and Kharaka, Y.K. (1976) Hydrogen and oxygen isotope exchange reactions between clay minerals and water. Geochimica et Cosmochimica Acta, 40, 241–246.

Phillips, T.L., Loveless, J.K., and Bailey, S.W. (1980) Cr^{+3} coordination in chlorites: A structural study of ten chromian chlorites. American Mineralogist, 65, 112–122.

Richet, P., Roux, J., and Pineau, F. (1986) Hydrogen isotope fractionation in the system H_2O-liquid-$NaAlSi_3O_8$: New data and comments on D/H fractionation in hydrothermal experiments. Earth and Planetary Science Letters, 78, 115–120.

Rye, R.O., Schuiling, R.D., Rye, D.M., and Jansen, J.B.H. (1976) Carbon, hydrogen and oxygen isotope studies of the regional metamorphic complex at Naxos, Greece. Geochimica et Cosmochimica Acta, 40, 1031–1049.

Sakai, H., and Tsutsumi, M. (1978) D/H fractionation factors between serpentine and water at 100 to 500°C and 2000 bar water pressure, and the D/H ratios of natural serpentines. Earth and Planetary Science Letters, 40, 231–242.

Satake, H., and Matsuda, J. (1979) Strontium and hydrogen isotope geochemistry of fresh and metabasalt dredged from the Mid-Atlantic Ridge. Contributions to Mineralogy and Petrology, 70, 153–157.

Satake, H., and Matsuo, S. (1984) Hydrogen isotopic fractionation factor between brucite and water in the temperature range from 100° to 500°C. Contributions to Mineralogy and Petrology, 86, 19–24.

Shannon, E.V., and Wherry, E.T. (1922) Notes on white chlorites. Journal of the Washington Academy of Sciences, 12, 239–241.

Sheppard, S.M.F. (1977) Identification of the origin of ore-forming solutions by the use of stable isotopes. In Volcanic processes in ore genesis, p. 25–41. Institution of Mining and Metallurgy and Geological Society, London.

——— (1980) Isotopic evidence for the origins of water during metamorphic processes in oceanic crust and ophiolite complexes. In Association mafiques ultra-mafiques dans les orogenes. Colloques Internationaux du C.N.R.S., 272, 135–147.

Stakes, D.S., and O'Neil, J.R. (1982) Mineralogy and stable isotope geochemistry of hydrothermally altered oceanic rocks. Earth and Planetary Science Letters, 57, 285–304.

Suzuoki, T., and Epstein, S. (1976) Hydrogen isotope fractionation between OH-bearing minerals and water. Geochimica et Cosmochimica Acta, 40, 1229–1240.

Taylor, H.P. (1974) The application of oxygen and hydrogen isotope studies to problems of hydrothermal alteration and ore deposition. Economic Geology, 60, 843–883.

Velde, B., and Rumble, D. (1977) Alumina content of chlorite in muscovite-bearing assemblages. Carnegie Institution of Washington Year Book 76, 621–623.

Viglino, J.A., Graham, C.M., and Harmon, R.S. (1984) Experimental hydrogen isotope fractionation factors in the system chlorite-H_2O. Geological Society of America Abstracts with Programs, 16, 683.

Wenner, D.B., and Taylor, H.P. (1973) Oxygen and hydrogen isotope studies of the serpentinization of ultramafic rocks in oceanic environments and continental ophiolites. American Journal of Science, 273, 207–239.

MANUSCRIPT RECEIVED NOVEMBER 5, 1985
MANUSCRIPT ACCEPTED FEBRUARY 13, 1987